

AdaZoom: Adaptive Zoom Network for Multi-Scale Object Detection in Large Scenes

Jingtao Xu Yali Li Shengjin Wang

Department of Electronic Engineering, Tsinghua University

xjd19@mails.tsinghua.edu.cn liyali13, wsgsj@tsinghua.edu.cn

Abstract

Detection in large-scale scenes is a challenging problem due to small objects and extreme scale variation. It is essential to focus on the image regions of small objects. In this paper, we propose a novel Adaptive Zoom (AdaZoom) network as a selective magnifier with flexible shape and focal length to adaptively zoom the focus regions for object detection. Based on policy gradient, we construct a reinforcement learning framework for focus region generation, with the reward formulated by object distributions. The scales and aspect ratios of the generated regions are adaptive to the scales and distribution of objects inside. We apply variable magnification according to the scale of the region for adaptive multi-scale detection. We further propose collaborative training to complementarily promote the performance of AdaZoom and detection network. To validate the effectiveness, we conduct extensive experiments on VisDrone2019, UAVDT and DOTA datasets. The experiments show AdaZoom brings consistent and significant improvement over different detection networks, achieving state-of-the-art performance on these datasets, especially outperforming the existing methods by AP of 4.64% on VisDrone2019.

1. Introduction

In recent years, significant progress has been achieved in computer vision. Visual object detection has also been extensively studied since it is important in various applications such as video surveillance and autonomous driving. Existing detectors such as Faster R-CNN [33], YOLO [32], and CornerNet [18] achieve satisfying performance on natural images. However, in practical applications such as Unmanned Aerial Vehicle (UAV) vision, existing detectors perform poorly because the images capture large-scale scenes with wide fields of view and quite small objects.

There are several challenges for detecting objects in large-scale scenes: (1) Objects are small and dense. For ex-

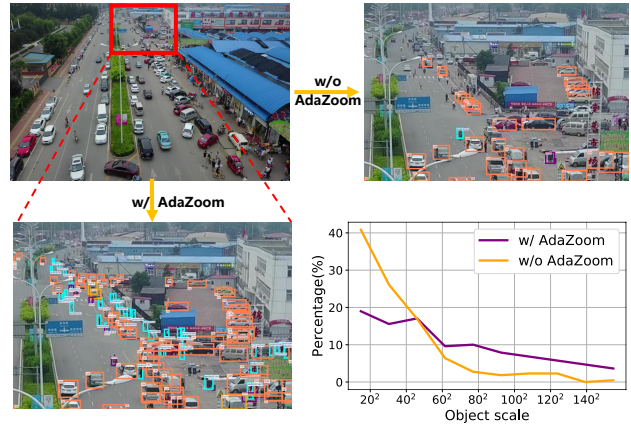


Figure 1. In large-scale images such as UAV images, objects are small and dense. AdaZoom works as a selective magnifier to generate and zoom the focus regions for further detection. The line chart presents the distribution of object scales in the image with and without focus regions generated by AdaZoom, respectively.

ample, the UAV takes images from high altitude with wide field of view, as shown in Fig. 1. Tens and hundreds of objects exist in a single image and most of them occupy quite a few pixels. Deep neural network with successive down-sampling would bring intolerable loss for semantic and positional information of small objects, resulting in poor detection performance. (2) Extreme scale variation across objects arises since images of large-scale scenes record a large span of distance and the camera-object distance varies significantly. Objects become smaller with further distance. Even objects of the same category may differ hundred times in scale. However, the receptive field of convolutional neural networks is limited. Extreme scale variation results in semantic gaps in convolution layers and brings substantial burdens in learning the powerful feature representations.

To tackle the object detection in large-scale scenes, it is urgent to design an adaptive zoomer to “focus” on objects with varying scales. Although there are some works on resizing images for multi-scale training [35, 36] and inference

on enlarged image crops [10, 30, 42], they are inflexible for objects of various scales in large-scale scenes and separate training and inference into different pipelines.

We propose an Adaptive Zoom (AdaZoom) network based on policy gradient [37] to adaptively zoom the focus regions for further detection. Inspired by human perception [29], when we perceive a large-scale scene, we glance over the whole image for coarse cognition and zoom where objects are small and dense for a careful watch.

AdaZoom works as a selective magnifier with flexible shape and focal length. It focuses on image regions with small objects. The scale and aspect ratio of the region to be zoomed are adaptive to the scales and distribution of objects inside. For a cluster of smaller objects, AdaZoom prefers a smaller focus region enclosing them for higher magnification, just like using a magnifier with shorter focal length. Without additional annotations for regions, AdaZoom is optimized according to the reward which measures the quality of the focus region. Following the paradigm of deep reinforcement learning, we further learn the policy network to produce focus regions with the regard of visual features. In addition, we design collaborative training to iteratively promote the joint training performance of AdaZoom and the detector. The outputs of detector are introduced to the reward which guides AdaZoom to focus on difficult regions. Then the regions generated by AdaZoom will be zoomed for finetuning the detector. With collaborative training, the detection performance is further improved consistently and significantly.

In summary, the main contributions are as follows:

- We propose a novel Adaptive Zoom (AdaZoom) network to adaptively generate and zoom the focus regions for accurate detection in large scenes, without additional annotations for the regions.
- We propose collaborative training to jointly boost the coordination between AdaZoom and the detector with a consistent pipeline of training and inference.
- Without bells and whistles, AdaZoom achieves state-of-the-art on the VisDrone2019 [47], UAVDT [9] and DOTA [41] datasets.

2. Related work

Multi-scale object detection. Multi-scale training and inference with image pyramid is the most straightforward idea to alleviate the problem of small objects [7, 11, 16, 34]. However, the image pyramid increases the scale variation of images. SNIP [35] proposes a training paradigm ignoring objects out of the desire size range during gradient back-propagation. Following the idea of [35], SNIPER [36] focuses on efficient multi-scale training by sampling chips of different sizes. These chips are resized to a certain

size for multi-scale training. Further, AutoFocus [30] extends SNIPER [36] to a coarse-to-fine pipeline that predicts regions of interest at a coarse level and then infers on the regions at a fine level. In addition, DREN [44] and ClusDet [42] employ neural networks to estimate difficult regions for fine detection. However, these methods separate multi-scale training and inference into different pipelines which leads to inconsistency between training and inference. Apart from multi-scale process in image level, another direction is to build pyramid in feature level [13, 15, 21, 23, 24]. Feature Pyramid Network [21] is widely utilized in many SOTA detectors for cross-layer feature fusion. Due to the limitation of the receptive field of convolutional neural networks, [3, 24] assign smaller objects to shallower layers. Our method focuses on image level. We introduce deep reinforcement learning into adaptive region generation for multi-scale object detection and integrate the training and inference into the same pipeline with the regions generated by AdaZoom.

Reinforcement-learning-based object detection. Reinforcement learning is introduced to object detection in the following ways: (1) Focusing on objects step by step with accumulated evidence [2, 5, 12, 14, 20, 43]. In particular, an image contains specific context information and a sequence process accumulates evidence from context for detection. [12] learns a search strategy to collect context and select the next window to visit. In addition, objects in the same scene have relationship with each other, such as a person riding on a bicycle. The detected objects provide contextual cues for subsequent steps of detection [17]. (2) Selecting high-quality regions of interest. [28] proposes a sequential exploration process to select region proposals. [31] introduces deep reinforcement learning into region proposal network to filter out low-quality proposals and accumulate class-specific evidence over time step to boost detection accuracy. Besides, several works [10, 26, 38] propose selection strategies to acquire image regions from enormous candidates. Sharing the similar idea, we go beyond in the adaptability of region generation and propose effective collaborative training for region generation and detection.

3. Method

3.1. Analysis of Focus Adaptability

For effective object detection in large-scale scenes, it is essential to focus on the object-centric regions. The Uniform Partition (UP) is a straightforward strategy to “focus” on image regions in a sliding-window way. It partitions an image into several uniform regions and enlarges those regions for detection. We first conduct the UP strategy on the VisDrone2019 [47] for analysis. Various settings of UP (1×1 , 2×2 , 3×3 , 4×4) and all the combinations are evaluated ($n \times m$ denotes uniformly partitioning the image

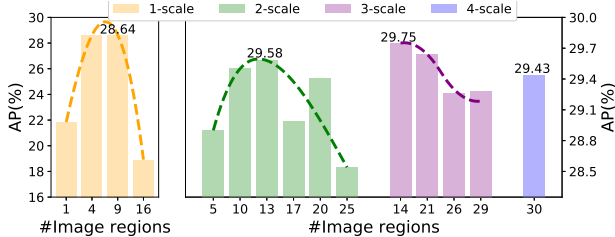


Figure 2. The average precision of uniform partition with different scales and their combinations on VisDrone2019 dataset. The UP of appropriate settings improves the AP and multi-scale UP further improves the detection accuracy. However, when the number of regions increases, the detection accuracy drops notably.

into $n \times m$ regions). The detection accuracy measured by average precision (AP) is presented in Fig. 2. The UP of appropriate settings does improve the AP, which validates the importance of focus regions in large scenes. Compared to single-scale setting (Fig. 2 left), multi-scale UP would further improve the detection accuracy (Fig. 2 right). However, when the number of regions increases, the detection accuracy drops notably. That is because the false negatives accumulate with the multi-scale repeated partitioned regions. Besides, with more cropped regions, the possibility of objects truncated by additional cropping is higher, which would cause more repeated and incomplete detections. Moreover, the UP strategy enlarges the cropped image regions with a fixed scale, which is inappropriate for scale-adaptive object detection in large scenes. In a word, the performance of UP strategy is limited by the lacking of adaptivity issue.

To tackle this, it is essential to adaptively generate focus regions in large-scene images for effective and efficient detection. Yet it is difficult to label the focus regions as true or false since the semantics is ambiguous. This makes it difficult to learn the designed network in supervised learning scheme. Based on these considerations, we propose an Adaptive Zoom network (AdaZoom) based on reinforcement learning (RL), as shown in Fig. 4. We design a continuous reward to measure the quality of focus regions based on the scales and distribution of objects. The RL agent is then encouraged to explore an adaptive region generation policy which maximizes the accumulated reward. In particular, AdaZoom can localize and zoom the focus regions with flexible shape and scale. The focus regions are adaptive to the scales and distribution of objects, which can significantly alleviate the scale variation towards high-performance object detection in large scenes.

3.2. Problem Formulation

We construct AdaZoom with reinforcement learning framework. Based on policy gradient [37], AdaZoom is optimized according to the reward which measures the quality

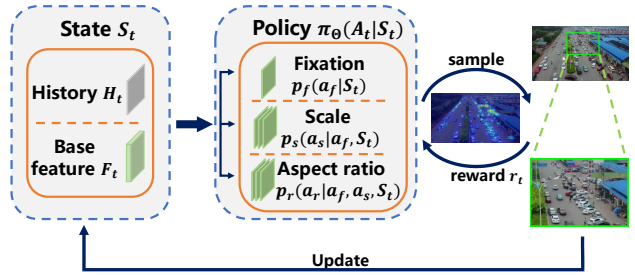


Figure 3. Formulation of focus region generation. The state S_t is composed of base feature F_t and history information map H_t . The action A_t is decoupled to the fixation a_f , scale a_s and aspect ratio a_r of focus regions. Object distribution is introduced into the sampling process. The reward is derived from object distribution.

of the focus region. We view the sequence of region generation as a Markov Decision Process (MDP) [1] and formulate adaptive focus region generation as a reinforcement learning problem. As shown in Fig. 3, we construct the Policy Network π_Θ to generate the probability distribution of action space based on the state S_t . The action A_t is decoupled into fixation, scale, and aspect ratio of the focus region. The object distribution is referred to guide the sampling process for better convergence. Then we derive the reward r_t from object distribution to measure the quality of a region. The state S_{t+1} is updated according to the generated region. For each image, T time steps make up an episode and we optimize the AdaZoom with policy gradient [37] to maximize the expected cumulative reward of each episode.

State. The state S_t consists of the base feature map F_t and the history information map H_t . F_t is supposed to learn the object-wise scale and distribution information at a coarse level. It is distinct from the feature maps for object detection which focus on the fine-level features of each object. The binary history information map H_t records the regions generated at previous steps. The initial state S_0 is the concatenation of an all-zero binary map H_0 and the base feature map F_0 which is extracted from the image by a backbone network. The focus region is mapped from the image to the state, denoted as z_t . The state is updated as follows:

$$H_{t+1}(i, j) = \mathbb{I}\{(i, j) \in z_t\} + H_t(i, j)\mathbb{I}\{(i, j) \notin z_t\} \quad (1)$$

$$F_{t+1}(i, j) = \kappa F_t(i, j)\mathbb{I}\{(i, j) \in z_t\} + F_t(i, j)\mathbb{I}\{(i, j) \notin z_t\} \quad (2)$$

where $\mathbb{I}(\cdot)$ is the indicator function and κ is a decay factor to suppress the response in the corresponding focus region. We set κ to 0.1.

Action. The action A_t is sampled from the probability distribution $\pi_\Theta(A_t|S_t)$. We design a three-branch Policy Network to progressively learn the fixation, scale and aspect ratio of focus regions. The first branch generates the probability distribution for fixation $p_f(a_f|S_t)$, where a_f is

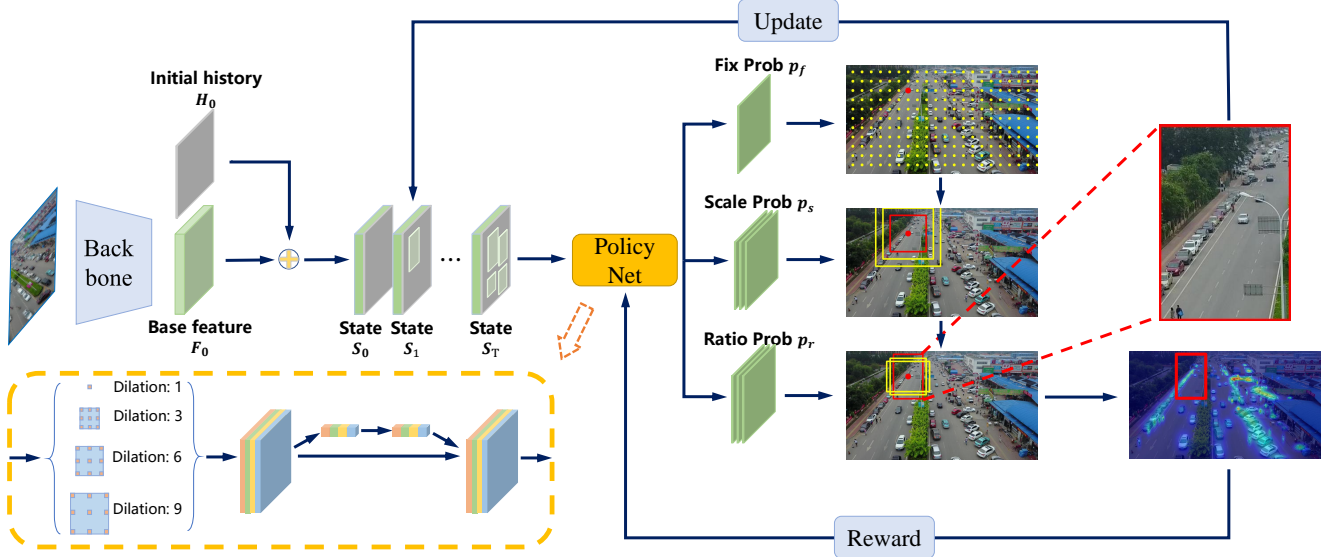


Figure 4. The workflow of AdaZoom. The initial state S_0 is composed of base feature F_0 and history information map H_0 . F_0 is extracted from the image and the values of H_0 are all set to zero. The PolicyNet generates three branches for the probability of fixation, scale, and aspect ratio, respectively. The focus region is sampled from these probability maps. Then the state S_1 is updated for the next time step according to the focus region. The reward of the focus region is derived from the object distribution.

a point on the fixation probability map $p_f \in \mathbb{R}^{h \times w}$. Inspired by the anchor based mechanism [33], each point in the fixation probability map represents a region center location in the image. The second branch generates a scale probability map $p_s \in \mathbb{R}^{h \times w \times n_s}$, where n_s is the predefined number of candidate region scales. $p_s(a_s|a_f; S_t)$ is conditioned on the fixation a_f , where a_s is the region scale. The third branch generates aspect ratio probability map $p_r \in \mathbb{R}^{h \times w \times n_s \times n_r}$, where n_r is the predefined number of candidate aspect ratios. The aspect ratio probability distribution $p_r(a_r|a_f, a_s; S_t)$ is conditioned on the fixation a_f and scale a_s . The action A_t is composed of (a_f, a_s, a_r) to specify a region. We formulate the policy as follows:

$$\pi_{\Theta}(A_t|S_t) = p_f(a_f|S_t) \times p_s(a_s|a_f; S_t) \times p_r(a_r|a_f, a_s; S_t) \quad (3)$$

These branches coordinate with each other by focusing on region representation from different points of view. The fixation branch tries to find the center of a cluster of objects. The scale branch is supposed to adjust the scale of the region according to the scales of objects around the fixation. The aspect ratio branch adapts to the distribution of objects around the fixation with a selected scale of the region. The network structure is detailed in the Supplementary Material.

Reward. There are no clear annotations to supervise the region generation since the image can be partitioned into reasonable regions in many ways and the semantics of the region is ambiguous for supervised learning. Therefore, we design the reward which measures the quality of the regions. The reward is derived from annotations for bound-

ing boxes of objects. AdaZoom is expected to pay more attention to small objects. For the i_{th} object, it is assigned a weight $w_i \propto \frac{1}{s_i}$, where s_i is the scale of the object. For each scale a_s of region, there is a desired object scale range $[a_s^{min}, a_s^{max}]$. The reward at step t is defined as follows:

$$r_t(A_t) = \frac{\sum_{Z_t} I_i(a_s) w_i}{\sum_{\tilde{Z}} w_j} \quad (4)$$

where Z_t is the set of objects enclosed in the t_{th} focus region and \tilde{Z} corresponds to the remaining regions of the image until step $t - 1$. In general, r_t can be regarded as a weighted recall of object weights w at step t . $I_i(a_s)$ denotes the measurement of consistency between scales of objects and regions. For the i_{th} object in the focus region with a_s scale, if the scale of the object falls beyond $[a_s^{min}, a_s^{max}]$, w_i will decay by $I_i(a_s)$ and the mismatch between the scale of the region and object is introduced to reward. $I_i(a_s)$ is defined as follows:

$$I_i(a_s) = \begin{cases} 1, & s_i \in [a_s^{min}, a_s^{max}] \\ \max(0, 2 - e^{\beta \Delta s}), & otherwise \end{cases} \quad (5)$$

where s_i is the scale of the object, $\Delta s = \frac{|s_i - a_s^{min(max)}|}{a_s^{min(max)}}$ is the fraction that s_i exceeds a_s^{max} or smaller than a_s^{min} . β is a positive coefficient to adjust the decay rate for scales beyond scale range. we set β to 1.5.

3.3. Training and Inference

Our approach for object detection in large-scale scenes contains two components: (1) AdaZoom network to adapt-

tively zoom the focus regions; (2) Detection network to locate the objects in focused regions. We train AdaZoom and detection network collaboratively to boost the performance.

Collaborative training. AdaZoom generates a series of focus regions with different scales and aspect ratios. We crop these focus regions from the original image and resize them to a certain scale so that smaller regions obtain higher magnification. In order to alleviate the domain shift between original images and resized regions, the detector is re-trained on the resized regions. Different from the existing work [10, 30, 36], we integrate the training and inference in the same pipeline with the focus regions generated by AdaZoom. In addition, we design collaborative training to further improve the performance of detection. During collaborative training, AdaZoom is expected to focus on the regions difficult for the re-trained detector. The detector infers on the image and outputs confidence scores c_i for each object. For false negative, the confidence score is set to zero. Then the weight w_i in Eq. 4 is modified as $w_i = 1 - c_i$. The AdaZoom is trained on the new modified weights. As a consequence, AdaZoom pay attention to difficult regions where the confidence of true positive is low. Then the difficult regions generated by the AdaZoom are used to finetune the detector (Fig. 5). This simple modification promotes the coordination between AdaZoom and the detector.

Inference. Inference shares the same pipeline with training. We adopt the greedy sampling to take actions:

$$\begin{cases} a_f = \arg \max_{a_f} p_f(a_f | S_t) \\ a_s = \arg \max_{a_s} p_s(a_s | a_f; S_t) \\ a_r = \arg \max_{a_r} p_r(a_r | a_f, a_s; S_t) \end{cases} \quad (6)$$

The fixation a_f is selected as the center of regions. Conditioned on fixation a_f , AdaZoom selects a scale a_s that implies the scales of objects around fixation. With the selected fixation a_f and scale a_s , an aspect ratio a_r is selected to adapt to the distribution of objects around fixation. Based on the selected actions, a region is generated. The generated regions as well as the original image are resized together to a certain scale as a batch for detection. The final results of each region are merged together by non-maximum suppression(NMS) with the IoU threshold setting to 0.5.

4. Experiments

4.1. Dataset and Metric

We conduct experiments on the public detection benchmark VisDrone2019 [47], UAVDT [9] and DOTA [41] to evaluate our method. (1) **VisDrone2019** [47] consists of 10,209 images for detection task with *train* set of 6,471 images, *val* set of 548 images. The *test* set is split into *test-dev* with 1,610 images and *test-challenge* with 1,580 images.

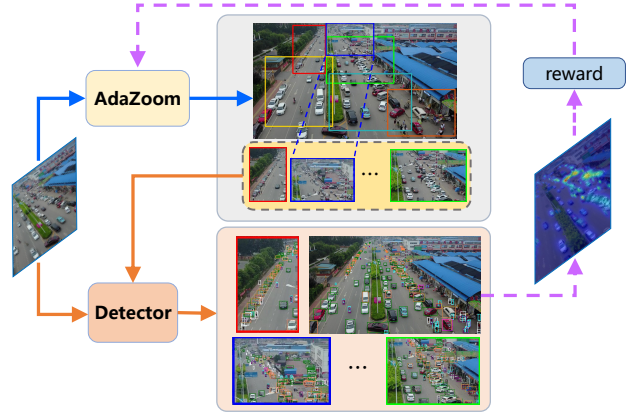


Figure 5. When training the detector, the focus regions generated by AdaZoom are resized to a certain scale to finetune the detector. When training AdaZoom, the detection results of the image are introduced to the reward for AdaZoom. During inference, the final detection results are merged from focus regions and the image.

The resolution of images can be as large as 2000×1500 pixels. On average, each image has 53 objects and most of them are small as well as densely distributed. (2) **UAVDT** [9] is another popular UAV-based detection benchmark. It consists of 23258 training images and 15069 testing images. The average resolution of images is about 1080×540 pixels. The tiny objects just contain 0.005% pixels of a frame. (3) **DOTA** [41] is a public dataset for remote sensing. There are 1411 images for training and 458 images for validation. Following ClusDet [42], we choose the images with movable objects such as plane, ship, vehicle and helicopter. The dataset contains 920 images for training and 285 images for validation.

We follow the evaluation COCO-style protocol in [47] with the official evaluation toolkit¹ for VisDrone2019. We also use the evaluation protocol in COCO [22] for UAVDT and DOTA. The detection performance is evaluated with metrics of $AP^{[0.5:0.05:0.95]}$, $AP^{0.5}$, $AP^{0.75}$.

4.2. Implementation Details

For AdaZoom, we set $n_s = 3$ for scale candidates $[240^2, 350^2, 420^2]$ and the desired scale ranges are set to $(0, 40^2), (30^2, 60^2), (50^2, \infty)$, respectively. The candidate aspect ratios are $[0, 7, 1.0, 1.5]$. The max step number per episode T is set to 7, empirically. We train the AdaZoom with 16 batch size and $2e-5$ learning rate for 5k iterations. For the detector (*i.e.*, Faster R-CNN [33] and Cascade R-CNN [4]), we follow the default configurations of maskrcnn-benchmark [27]. We train the detector for 90k iterations with 0.001 learning rate. The learning rate is decreasing by a factor of 0.1 after 60k iterations and 80k iterations. During training and inference, the short edge of re-

¹<https://github.com/VisDrone/VisDrone2018-DET-toolkit>

Dataset	Method	AP	AP_{50}	AP_{75}	s/img(GPU)
VisDrone2019	UP(1 × 1)	21.84	40.92	21.46	0.070
	UP(2 × 2)	28.61	51.97	28.34	0.270
	UP(3 × 3)	28.64	52.70	27.90	0.617
	Multi-Ratio UP	29.01	52.99	28.46	1.078
	Multi-Scale UP	29.75	53.89	29.56	0.960
	AdaZoom	31.22	56.16	31.22	0.654
UAVDT	UP(1 × 1)	12.1	23.5	10.8	0.067
	UP(2 × 2)	13.3	25.1	13.1	0.252
	UP(3 × 3)	10.9	21.3	9.9	0.558
	Multi-Ratio UP	15.0	27.3	15.3	1.008
	Multi-Scale UP	15.3	28.1	15.4	0.854
	AdaZoom	19.6	33.6	21.3	0.599

Table 1. Comparison with uniform partition on VisDrone2019 *test-dev* and UAVDT *test* dataset. We adopt Faster R-CNN as the detector. We also report the inference time per image.

Method	Backbone	AP	AP_{50}	AP_{75}
Faster R-CNN [21]	ResNet50	12.1	23.5	10.8
ClusDet [42]	ResNet50	13.7	26.5	12.5
DMNet [19]	ResNet50	14.7	24.6	16.3
DREN [44]	ResNet50	15.1	-	-
GLSAN [8]	ResNet50	17.0	28.1	18.8
GLSAN† [8]	ResNet50	19.0	30.5	21.7
AdaZoom	ResNet50	19.6	33.6	21.3
AdaZoom†	ResNet50	22.4	38.6	23.9
Faster R-CNN [21]	ResNet101	15.1	26.5	16.0
GLSAN [8]	ResNet101	17.1	28.3	18.8
DREN [44]	ResNet101	17.7	-	-
AdaZoom	ResNet101	20.1	34.5	21.5

Table 2. Detection performance on UAVDT *test* dataset. We adopt Faster R-CNN and Cascade R-CNN as the detector. † denotes Cascade R-CNN.

gions generated by AdaZoom are resized to 800 pixels. For collaborative training, we iteratively finetune AdaZoom for 500 iterations and detector for 1000 iterations with learning rate decayed by 0.1.

4.3. Comparison with Baseline

We first compare the proposed AdaZoom with the Uniform Partitions (UP) as the baseline, to evaluate the effectiveness. For UP, a whole image is uniformly partitioned into $m \times n$ regions with 50 pixels overlap. In particular, we implement comprehensive experiments of UP to provide a simple yet strong baseline. We evaluate multi-scale UP of $[1 \times 1, 2 \times 2, 3 \times 3]$ and multi-ratio UP of $[2 \times 3, 2 \times 2, 3 \times 2]$. Table 1 shows the comparative study with Faster R-CNN as the detector and ResNet-50 backbone. On VisDrone2019 dataset, the AdaZoom achieves AP of 31.22% and AP_{50} of 56.16%. Compared to UP of 3×3 , the AdaZoom improves AP by 2.58% with comparable inference time. Compared to the multi-scale UP and multi-ratio UP, the AdaZoom improves the AP by 1.47% \sim 2.21% and AP_{50} by 2.27% \sim 3.17%. On UAVDT dataset, the AdaZoom achieves AP of 19.6% and AP_{50} of 33.6%, outperforming UP by a large margin. Compared to multi-scale UP and

Method	Backbone	AP [%]	AP_{50} [%]	AP_{75} [%]
RRNET [6]	Hourglass	32.92	-	31.33
CRENet [40]	Hourglass-104	33.70	54.30	33.50
DMNet [19]	ResNet50	28.20	47.60	28.90
CascadeNet [45]	ResNet50	30.12	58.02	27.53
GLSAN [8]	ResNet50	30.70	55.40	30.00
SAMFR [39]	ResNet50	33.72	58.62	33.88
MPPFN [25]	ResNet101	29.05	54.38	26.99
GLSAN [8]	ResNet101	30.70	55.60	29.90
ClusDet [42]	ResNeXt101	32.40	56.20	31.60
SAIC-FPN [46]	ResNeXt101	35.69	62.97	35.08
DREN [44]	ResNeXt152	30.30	-	-
w/o CT:				
AdaZoom	ResNet50	34.71	62.16	33.89
AdaZoom	ResNeXt101	36.56	64.58	36.03
AdaZoom†	ResNeXt101	38.69	65.35	39.45
w/ CT:				
AdaZoom	ResNet50	36.19	63.50	36.11
AdaZoom	ResNeXt101	37.58	66.25	37.34
AdaZoom†	ResNeXt101	40.33	66.94	41.77

Table 3. Detection performance on VisDrone2019 *val* dataset. Results for SOTA are taken from the publications. We adopt Faster R-CNN and Cascade R-CNN as the detector following AdaZoom and † denotes Cascade R-CNN. We report the results with and without collaborative training (CT), respectively.

multi-ratio UP, we improve AP by 4.3% \sim 4.6% and AP_{50} by 5.5% \sim 6.3%, respectively. Meanwhile, compared to multi-scale UP, we save the 31.8% and 29.8% of inference time on VisDrone2019 and UAVDT dataset, respectively. The results validate that the proposed AdaZoom is both effective and efficient of object detection in large scenes. That is mainly because our method generates focus regions in an adaptive way. Instead of sliding over the whole image, we only generate the important regions with appropriate scales and shapes. Therefore, our method is adaptive to scale varying. Besides, the AdaZoom would avoid generating too many regions, further leading to notable accuracy boosting and inference time saving.

4.4. Comparison with State-of-The-Art Models

We compare our method with the state-of-the-art methods across a wide range of datasets, such as UAVDT *test* (Table 2), VisDrone2019 *val* (Table 3) and DOTA *val* dataset (Table 4). From the tables we can see that our method achieves superior performance over existing methods on all the three datasets. On UAVDT dataset, we achieve 22.4% of AP and 38.6% of AP_{50} with Cascade R-CNN as the detector. Compared to GLSAN [8] with Cascade R-CNN, the AP is increased by 3.4% and AP_{50} is increased by 8.1%. On Visdrone dataset, the AdaZoom achieves 40.33% and AP_{50} of 66.94%, outperforming the SOTA performance by a large margin. On DOTA dataset, we follow the experimental setting as [42] to evaluate the detection performance in large scenes. We achieve 37.8% of AP and 63.5% of AP_{50} , with ResNeXt-101 as backbone

Method	Backbone	AP	AP_{50}	AP_{75}
Faster R-CNN [21]	ResNet50	30.60	52.10	31.30
ClusDet [42]	ResNet50	32.20	47.60	39.20
AdaZoom	ResNet50	36.00	62.70	37.00
Faster R-CNN [21]	ResNet101	30.50	52.10	31.00
ClusDet [42]	ResNet101	31.60	47.80	38.20
AdaZoom	ResNet101	36.10	63.10	36.20
Faster R-CNN [21]	ResNeXt101	32.30	54.50	33.30
ClusDet [42]	ResNeXt101	31.40	47.10	37.40
AdaZoom	ResNeXt101	37.80	63.50	39.20

Table 4. Detection performance on DOTA *val* dataset. We adopt Faster R-CNN as detector and employ different backbones.

and Faster R-CNN as the detector. The achieved AP is increased by 5.5% \sim 6.4%. We also focus on the comparison with the existing methods which apply the cropped and resized regions for detection boosting, as follows.

Comparison with pseudo annotation based region generation methods. For such methods, pseudo annotations of focus regions are produced with the object annotations. Typically, ClusDet [42] trains a region generation network by supervised learning based on pseudo generated annotations. For fair comparison, we use the Faster R-CNN with the same backbone with the ClusDet. On Visdrone dataset, our method outperforms ClusDet by 4.16% in AP even without collaborative training. It is reasonable since the region selection is difficult to be formulated as a supervised learning problem. Assigning the hard labels as true or false to focus regions is semantically vague. In contrast, we design a continuous reward to measure whether a generated region is good or bad. The RL formulation is more suitable for such problem. In addition, by integrating collaborative training, our method outperforms ClusDet in AP by 5.18% on VisDrone2019 and 5.9% on UAVDT dataset. On DOTA [41] dataset, we set the number of focus regions of AdaZoom to 3. It should be noted from Table. 4 that our method achieves consistent improvement with stronger backbone.

Comparison with coarse-to-fine detection methods. For such methods, the object distribution is estimated based on a coarse-level preview detection, such as DREN [44], CRENet [40] and GLSAN [8]. Compared to CRENet with backbone of Hourglass-104, Our AdaZoom with Faster RCNN achieves 2.49% higher in AP on VisDrone2019 with ResNet-50 backbone. Compared to DREN [44] and ResNet101, the AP is increased by 4.5% with ResNet-50 backbone and 2.4% with ResNet-101 backbone on UAVDT dataset. Compared with GLSAN [8], which uses extra super-resolution network for enlarging regions, our method outperforms it by 5.49% of AP on VisDrone2019. The performance of the coarse-to-fine methods is limited by the initial detection, which would cause the bias for region generation (*i.e.*, small objects are easily missed in coarse-level detection). In contrast, our AdaZoom cooperates well with

SR	CT	AP [%]	AP_{50} [%]	AP_{75} [%]
		29.74	54.06	29.48
	✓	29.99	54.21	29.86
✓		30.51	55.28	30.22
✓	✓	31.22	56.16	31.22

Table 5. Ablation for AdaZoom on VisDrone2019 *test-dev*. We adopt Faster R-CNN with ResNet50 as detector. **SR**: Scale and ratio adaptation. **CT**: collaborative training.

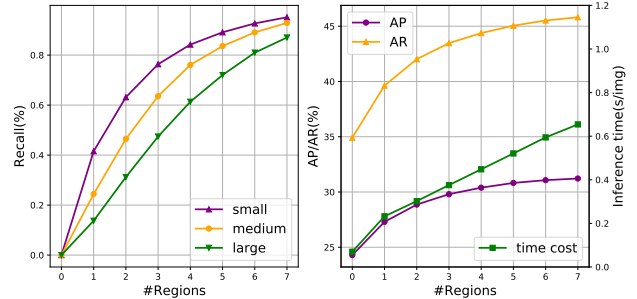


Figure 6. **Left**: recall curves for objects w.r.t. the number of focus regions. **Right**: AP/AR and inference time curves for the final detection performance on VisDrone2019 *test-dev* dataset w.r.t. the number of focus regions.

detector. The performance of both AdaZoom and detector are improved by collaborative training.

4.5. Ablation Study

There are two main components for AdaZoom network, such as adaptive generation of focus regions and collaborative training between AdaZoom and the detector. We evaluate the effects of different components on VisDrone2019 *test-dev* dataset. We use Faster R-CNN with ResNet50 for the ablation study, as shown in Table.5. SR denotes focus regions with adaptive scales of $[240^2, 350^2, 420^2]$ and adaptive aspect ratios of $[0.7, 1.0, 1.5]$. CT denotes collaborative training. The baseline uses the single scale of 350^2 and aspect ratio of 1.0 without collaborative training, achieving 29.74% in AP .

Effect of scale/ratio adaptation. The scale and ratio adaptation of focus regions achieves the dynamic multi-scale detection. The scale adaptation alleviate the problem of scale variation. The adaptation of aspect ratio improves the recall of objects with the limited number of regions. As Table.5 shows, SR stably improves the AP . In particular, compared with baseline, SR increases the flexibility and diversity in region generation which improves AP by 0.77%. Compared with the model with CT, SR further increased the AP by 1.23% and AP_{50} by 1.95%. The results prove that SR improves the performance of detection by adaptively zooming the focus regions with flexible scales and aspect ratios. The detector benefits from adaptive-scale detection.

Effect of collaborate training. CT optimizes the detec-

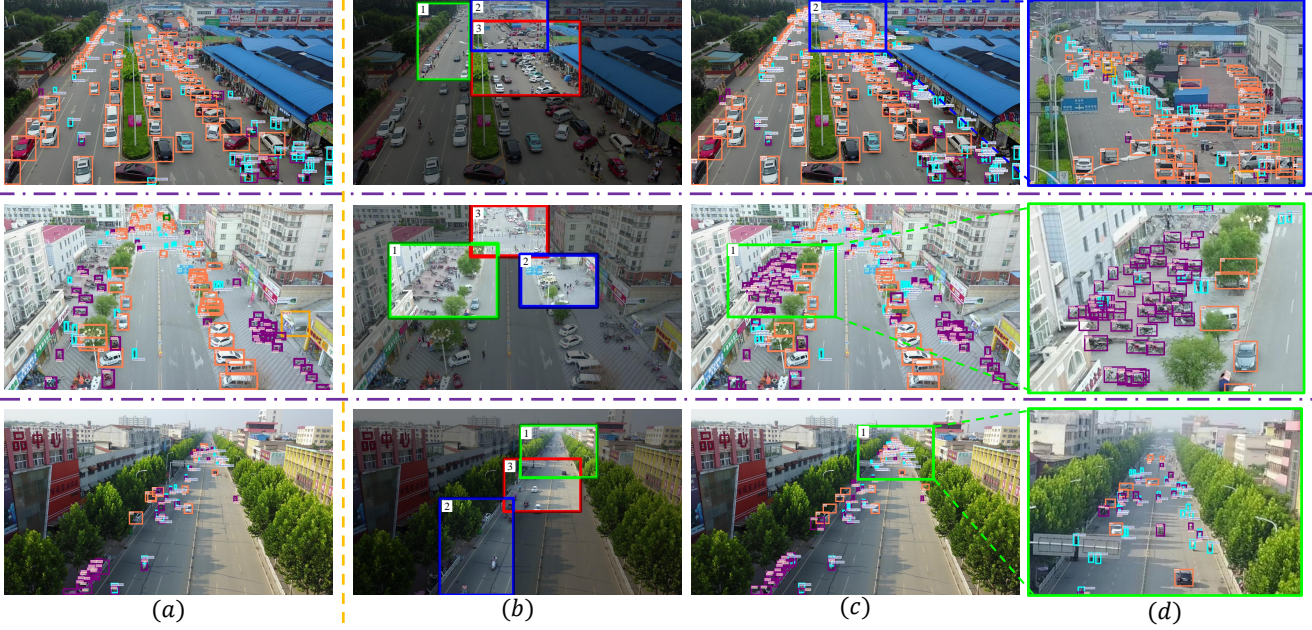


Figure 7. Visualizations of the performance of AdaZoom. (a) The detection results without AdaZoom. (b) The top-3 focus regions generated by AdaZoom. The focus regions adapt to the distribution and scales of objects. (c) The detection results with AdaZoom. The small and dense objects are also well detected. (d) The detection results on one of the focus regions. The results of (a) performs poorly on these regions.

tor with the focus regions generated by AdaZoom. Meanwhile, it guides AdaZoom to mine the fine-level regions for detector boosting with the reward based on detection results. Table.5 shows that CT gains consistent performance improvement under different settings. Compared to baseline, the CT slightly boosts the AP by 0.25% and AP_{75} by 0.38%, because the scale of regions keeps the same. The collaborate training loses the benefits from multi-scale detection. When combining with SR, CT gains performance improvement as 0.71% in AP and 1.00% in AP_{75} . The results show that involving collaboration between AdaZoom and the detector further promotes the object detection.

Effect of number of focus regions. The AdaZoom is motivated to adaptively propose focus regions with small and densely distributed objects, for further zoomed detection. To evaluate this, we present the recall rates (*i.e.*, the proportion of objects that are enclosed in the generated regions) for objects of the reinforcement-learning-based AdaZoom, as shown in Fig. 6 (left). For detailed analysis, we report the recall for *small*, *medium* and *large* objects, respectively. As can be seen in Fig. 6 (left), when the number of focus regions is 7, the recall of *small*, *medium* and *large* achieve 95.1%, 92.9%, and 87.0%, respectively. Recall of small objects increasing fastest at the beginning. Because AdaZoom pays more attention to small objects and it prefers to focus on the regions with small objects.

With detector of ResNet50-based Faster R-CNN, the AP and AR are presented in Fig. 6(right). When the number

of regions is zero, the detector is trained on the generated regions and infers on original images. The inference time almost linearly increases w.r.t. the number of focus regions. Our method can easily achieve the balance between accuracy and efficiency by setting the number of focus regions.

Qualitative evaluation. We visualize the detection results with and without AdaZoom in Fig. 7. We also display the top-3 focus regions for each image and the detection results on the focus regions. It can be observed from Fig. 7 (b) that the AdaZoom generates small region for small objects and the shape of the region adapts to the distribution of objects. Comparing Fig. 7 (c) with (a), the small and dense objects are well detected by our method, especially in the focus regions. Our method can adaptively focus on the important regions and achieve higher recalls of the small and dense objects.

5. Conclusion

In this work, we propose an Adaptive Zoom (AdaZoom) network to zoom the focus regions with flexible scale and aspect ratio for multi-scale object detection. We optimize AdaZoom with policy gradient algorithm without additional annotations for focus regions. Moreover, we propose collaborative training to promote the coordination between AdaZoom and the detector which further improves the performance of detection. Without bells and whistles, our method achieves state-of-the-art on the VisDrone2019, UAVDT and DOTA datasets.

References

- [1] Richard Bellman. A markovian decision process. *Journal of mathematics and mechanics*, pages 679–684, 1957. 3
- [2] Miriam Bellver, Xavier Giro-I-Nieto, Ferran Marques, and Jordi Torres. Hierarchical object detection with deep reinforcement learning. *Advances in Parallel Computing*, 31, 2016. 2
- [3] Zhaowei Cai, Quanfu Fan, Rogerio S Feris, and Nuno Vasconcelos. A unified multi-scale deep convolutional neural network for fast object detection. In *European conference on computer vision*, pages 354–370. Springer, 2016. 2
- [4] Zhaowei Cai and Nuno Vasconcelos. Cascade r-cnn: Delving into high quality object detection. In *Proceedings of the IEEE conference on computer vision and pattern recognition*, pages 6154–6162, 2018. 5
- [5] Juan C. Caicedo and Svetlana Lazebnik. Active object localization with deep reinforcement learning. In *2015 IEEE International Conference on Computer Vision (ICCV)*, 2015. 2
- [6] Changrui Chen, Yu Zhang, Qingxuan Lv, Shuo Wei, Xiaorui Wang, Xin Sun, and Junyu Dong. Rrnet: A hybrid detector for object detection in drone-captured images. In *Proceedings of the IEEE International Conference on Computer Vision Workshops*, pages 0–0, 2019. 6
- [7] Jifeng Dai, Yi Li, Kaiming He, and Jian Sun. R-fcn: Object detection via region-based fully convolutional networks. In *Advances in neural information processing systems*, pages 379–387, 2016. 2
- [8] Sutaog Deng, Shuai Li, Ke Xie, Wenfeng Song, Xiao Liao, Aimin Hao, and Hong Qin. A global-local self-adaptive network for drone-view object detection. *IEEE Transactions on Image Processing*, 2020. 6, 7
- [9] Dawei Du, Yuankai Qi, Hongyang Yu, Yifan Yang, Kaiwen Duan, Guorong Li, Weigang Zhang, Qingming Huang, and Qi Tian. The unmanned aerial vehicle benchmark: Object detection and tracking. In *Proceedings of the European Conference on Computer Vision (ECCV)*, pages 370–386, 2018. 2, 5
- [10] Mingfei Gao, Ruichi Yu, Ang Li, Vlad I Morariu, and Larry S Davis. Dynamic zoom-in network for fast object detection in large images. In *Proceedings of the IEEE Conference on Computer Vision and Pattern Recognition*, pages 6926–6935, 2018. 2, 5
- [11] Ross Girshick. Fast r-cnn. *Computer ence*, 2015. 2
- [12] Abel Gonzalez-Garcia, Alexander Vezhnevets, and Vittorio Ferrari. An active search strategy for efficient object class detection. In *Proceedings of the IEEE Conference on Computer Vision and Pattern Recognition*, pages 3022–3031, 2015. 2
- [13] Chaoxu Guo, Bin Fan, Qian Zhang, Shiming Xiang, and Chunhong Pan. Augfpn: Improving multi-scale feature learning for object detection. In *Proceedings of the IEEE/CVF Conference on Computer Vision and Pattern Recognition*, pages 12595–12604, 2020. 2
- [14] Kota Hara, Ming-Yu Liu, Oncel Tuzel, and Amir-massoud Farahmand. Attentional network for visual object detection. *arXiv preprint arXiv:1702.01478*, 2017. 2
- [15] Kaiming He, Xiangyu Zhang, Shaoqing Ren, and Jian Sun. Spatial pyramid pooling in deep convolutional networks for visual recognition. *IEEE Transactions on Pattern Analysis and Machine Intelligence*, 37(9):1904–16, 2014. 2
- [16] Kaiming He, Xiangyu Zhang, Shaoqing Ren, and Jian Sun. Deep residual learning for image recognition. In *2016 IEEE Conference on Computer Vision and Pattern Recognition (CVPR)*, 2016. 2
- [17] Xiangyu Kong, Bo Xin, Yizhou Wang, and Gang Hua. Collaborative deep reinforcement learning for joint object search. In *Proceedings of the IEEE Conference on Computer Vision and Pattern Recognition*, pages 1695–1704, 2017. 2
- [18] Hei Law and Jia Deng. Cornernet: Detecting objects as paired keypoints. In *Proceedings of the European Conference on Computer Vision (ECCV)*, pages 734–750, 2018. 1
- [19] Changlin Li, Taojiannan Yang, Sijie Zhu, Chen Chen, and Shanyue Guan. Density map guided object detection in aerial images. In *Proceedings of the IEEE/CVF Conference on Computer Vision and Pattern Recognition Workshops*, pages 190–191, 2020. 6
- [20] Yue Zhang Li, Katia Sycara, and Rahul Iyer. Object-sensitive deep reinforcement learning. *arXiv preprint arXiv:1809.06064*, 2018. 2
- [21] Tsung-Yi Lin, Piotr Dollár, Ross Girshick, Kaiming He, Bharath Hariharan, and Serge Belongie. Feature pyramid networks for object detection. In *Proceedings of the IEEE conference on computer vision and pattern recognition*, pages 2117–2125, 2017. 2, 6, 7
- [22] Tsung-Yi Lin, Michael Maire, Serge Belongie, James Hays, Pietro Perona, Deva Ramanan, Piotr Dollár, and C Lawrence Zitnick. Microsoft coco: Common objects in context. In *European conference on computer vision*, pages 740–755. Springer, 2014. 5
- [23] Shu Liu, Lu Qi, Haifang Qin, Jianping Shi, and Jiaya Jia. Path aggregation network for instance segmentation. In *Proceedings of the IEEE conference on computer vision and pattern recognition*, pages 8759–8768, 2018. 2
- [24] Wei Liu, Dragomir Anguelov, Dumitru Erhan, Christian Szegedy, Scott Reed, Cheng-Yang Fu, and Alexander C Berg. Ssd: Single shot multibox detector. In *European conference on computer vision*, pages 21–37. Springer, 2016. 2
- [25] Yingjie Liu, Fengbao Yang, and Peng Hu. Small-object detection in uav-captured images via multi-branch parallel feature pyramid networks. *IEEE Access*, 8:145740–145750, 2020. 6
- [26] Yongxi Lu, Tara Javidi, and Svetlana Lazebnik. Adaptive object detection using adjacency and zoom prediction. In *Proceedings of the IEEE Conference on Computer Vision and Pattern Recognition*, pages 2351–2359, 2016. 2
- [27] Francisco Massa and Ross Girshick. maskrcnn-benchmark: Fast, modular reference implementation of Instance Segmentation and Object Detection algorithms in PyTorch. <https://github.com/facebookresearch/maskrcnn-benchmark>, 2018. Accessed: [Insert date here]. 5
- [28] Stefan Mathe, Aleksis Pirinen, and Cristian Sminchisescu. Reinforcement learning for visual object detection. In *Pro-*

- ceedings of the IEEE Conference on Computer Vision and Pattern Recognition (CVPR)*, June 2016. 2
- [29] George W McConkie and Keith Rayner. The span of the effective stimulus during a fixation in reading. *Perception & Psychophysics*, 17(6):578–586, 1975. 2
- [30] Mahyar Najibi, Bharat Singh, and Larry S Davis. Autofocus: Efficient multi-scale inference. In *Proceedings of the IEEE International Conference on Computer Vision*, pages 9745–9755, 2019. 2, 5
- [31] Aleksis Pirinen and Cristian Sminchisescu. Deep reinforcement learning of region proposal networks for object detection. In *Proceedings of the IEEE Conference on Computer Vision and Pattern Recognition*, pages 6945–6954, 2018. 2
- [32] Joseph Redmon, Santosh Divvala, Ross Girshick, and Ali Farhadi. You only look once: Unified, real-time object detection. In *Proceedings of the IEEE conference on computer vision and pattern recognition*, pages 779–788, 2016. 1
- [33] Shaoqing Ren, Kaiming He, Ross Girshick, and Jian Sun. Faster r-cnn: Towards real-time object detection with region proposal networks. In *Advances in neural information processing systems*, pages 91–99, 2015. 1, 4, 5
- [34] Shaoqing Ren, Kaiming He, Ross Girshick, Xiangyu Zhang, and Jian Sun. Object detection networks on convolutional feature maps. *IEEE Transactions on Pattern Analysis and Machine Intelligence*, 39(7):1476–1481, 2017. 2
- [35] Bharat Singh and Larry S Davis. An analysis of scale invariance in object detection snip. In *Proceedings of the IEEE conference on computer vision and pattern recognition*, pages 3578–3587, 2018. 1, 2
- [36] Bharat Singh, Mahyar Najibi, and Larry S Davis. Sniper: Efficient multi-scale training. In *Advances in neural information processing systems*, pages 9310–9320, 2018. 1, 2, 5
- [37] Richard S. Sutton, David Mcallester, Satinder Singh, and Yishay Mansour. Policy gradient methods for reinforcement learning with function approximation. *Submitted to Advances in Neural Information Processing Systems*, 12, 1999. 2, 3
- [38] Burak Uzkent and Stefano Ermon. Learning when and where to zoom with deep reinforcement learning. In *Proceedings of the IEEE/CVF Conference on Computer Vision and Pattern Recognition*, pages 12345–12354, 2020. 2
- [39] Haoran Wang, Zexin Wang, Meixia Jia, Aijin Li, Tuo Feng, Wenhua Zhang, and Licheng Jiao. Spatial attention for multi-scale feature refinement for object detection. In *Proceedings of the IEEE International Conference on Computer Vision Workshops*, pages 0–0, 2019. 6
- [40] Yi Wang, Youlong Yang, and Xi Zhao. Object detection using clustering algorithm adaptive searching regions in aerial images. In *European Conference on Computer Vision*, pages 651–664. Springer, 2020. 6, 7
- [41] Gui-Song Xia, Xiang Bai, Jian Ding, Zhen Zhu, Serge Belongie, Jiebo Luo, Mihai Datcu, Marcello Pelillo, and Liangpei Zhang. Dota: A large-scale dataset for object detection in aerial images. In *Proceedings of the IEEE Conference on Computer Vision and Pattern Recognition*, pages 3974–3983, 2018. 2, 5, 7
- [42] Fan Yang, Heng Fan, Peng Chu, Erik Blasch, and Haibin Ling. Clustered object detection in aerial images. In *Proceedings of the IEEE International Conference on Computer Vision*, pages 8311–8320, 2019. 2, 5, 6, 7
- [43] Donggeun Yoo, Sunggyun Park, Joon Young Lee, Anthony S Paek, and In So Kweon. Attentionnet: Aggregating weak directions for accurate object detection. In *2015 IEEE International Conference on Computer Vision (ICCV)*, 2016. 2
- [44] Junyi Zhang, Junying Huang, Xuankun Chen, and Dongyu Zhang. How to fully exploit the abilities of aerial image detectors. In *Proceedings of the IEEE International Conference on Computer Vision Workshops*, pages 0–0, 2019. 2, 6, 7
- [45] Xindi Zhang, Ebroul Izquierdo, and Krishna Chandramouli. Dense and small object detection in uav vision based on cascade network. In *Proceedings of the IEEE International Conference on Computer Vision Workshops*, pages 0–0, 2019. 6
- [46] Jingkai Zhou, Chi-Man Vong, Qiong Liu, and Zhenyu Wang. Scale adaptive image cropping for uav object detection. *Neurocomputing*, 366:305–313, 2019. 6
- [47] Pengfei Zhu, Longyin Wen, Xiao Bian, Haibin Ling, and Qinghua Hu. Vision meets drones: A challenge. *arXiv preprint arXiv:1804.07437*, 2018. 2, 5